

# Viscosity of Komatiite Liquids at High Pressures

## Viscosity of Komatiite Liquids at High Pressures

Lara O'Dwyer Brown<sup>a</sup>, Charles E. Lesher<sup>b</sup>, Hidenori Terasaki<sup>b</sup>

<sup>a</sup> University of California at Davis; <sup>b</sup> Tohoku University

### INTRODUCTION

Mantle differentiation relies on the effective segregation of melts to facilitate fractionation, influencing the petrology of the Earth's interior and ultimately that of the surface. Viscosity is important as it controls the timescales for the segregation of melts from residues. Despite its importance our knowledge of viscosity and our ability to predict it are limited.

The viscosities of komatiite liquids at high pressures and temperatures were investigated using the in-situ falling sphere technique of BLD481, Shing-8. Komatiites are naturally occurring magmas, rich in network modifiers. They are derived from the early Earth's mantle and found in the rock record. Despite the refractory and fluid nature of komatiite, we successfully measured the viscosity of molten komatiites from Gorgona Island between 11 and 13 GPa at 2000 C, and from Beilngwe, Zimbabwe from 12 to 14 GPa at 2000 C.

### METHODS

Naturally occurring komatiite from Gorgona Island (GOR 94-29) and Beilngwe, Zimbabwe (B4) were chosen for this study (Table 1).

Table 1a. Chemical compositions of starting materials

	SiO <sub>2</sub>	TiO <sub>2</sub>	Al <sub>2</sub> O <sub>3</sub>	FeO	MnO	MgO	CaO	Na <sub>2</sub> O	K <sub>2</sub> O	Ti <sub>2</sub> O <sub>3</sub>	H <sub>2</sub> O
GOR 94-29	44.45	0.76	11.88	11.18	0.18	17.77	10.57	1.11	0.54	0.55	2.34
Nominally hydrated Anhydrous	44.71	0.76	11.93	11.54	0.18	17.88	10.51	1.12	0.54	0.55	2.00

Table 1b. NbO/T of starting materials

Sample	NbO/T
Gorgona Island (hydrated)	1.4
Gorgona Island (anhydrous)	1.8
Beilngwe, B4	2.1

We conducted in-situ falling sphere experiments at the BLD481 beamline at the SPiNG-8 (Figure 1). We generated pressure using SPEED-1500, a 1500 ton 2-stage millimeter-h. It has a DIA-type geometry with six outer anvils that compress eight tungsten carbide cubes. These cubes were cut with 8 mm truncations and were used with pressure media composed of MgO and ZrO<sub>2</sub> with corresponding edge lengths of 14 mm. Temperature was controlled using a D-type, W 35Re/ W 25% Re thermocouple (inserted axially). No correction was made for the effect of pressure on the thermocouple emf.

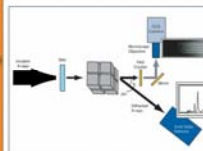


Figure 1. In the experimental hutch the X-Ray beam is fixed, and the press frame is mounted on a motorized table. This allows the sample to be centered for optimal X-ray radiography and diffraction. During experiments, X-rays are absorbed differentially in the sample. The outgoing beam is converted to visible light by a YAG (yttrium/aluminum/garnet) phosphor and then reflected by a mirror into a video camera, recording at 30 frames per second.

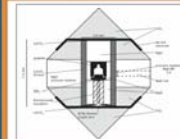


Figure 2. We used a double reservoir configuration for experiments, where a marker sphere was placed at the top of both the main melt reservoir and an overlying reservoir with a more refractory material, similar to the layered-capsule of Terasaki et al. (2001) and Liebske et al. (2005). This configuration allows the descent of two spheres at different temperatures. The starting material for each experiment was packed into the graphite capsules, and the Re marker spheres were completely surrounded with starting material.

Assemblies were first pressurized cold. Energy dispersive X-ray spectra for the pressure standard were collected at pressure, while the samples were cold and on heating. The settling velocities of the marker spheres were recorded in radiographs.

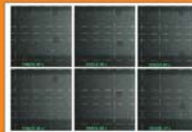


Figure 3a. Terminal Velocity of Falling Spheres: Using the motion tracking program MaxTRACQ, the sphere positions were determined relative to a scaled grid and frame numbers (30 frames per second). These radiographs show the lower sphere falling in experiment S2099, B4, at 12 GPa and between 1900 and 2000 C.

Figure 3b. These radiographs show the upper sphere falling in experiment S2099, B4, at 12 GPa and 2000 C.

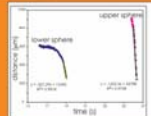


Figure 4. Time - distance profiles of two Re spheres in experiment S2099 on B4 at 12 GPa. The lower sphere falls between 1900 and 2000 C, the upper sphere falls at 2000 C. The terminal velocities of the Re spheres are defined by the slope of the linear section of the profile.

### RESULTS

The terminal velocities were used in Stokes' Law to calculate melt viscosities ( $\eta$ ):

$$\eta = \frac{2g r^2 \Delta \rho}{9 v_s}$$

where  $g$  is the gravitational constant,  $r$  is the radius of the sphere,  $\Delta \rho$  is the density contrast between the sphere and the melt,  $v_s$  is the settling velocity. The density of Re spheres at experimental conditions was calculated using equation of state parameters from Vohrer et al. (1987) and melt density was calculated from Lange and Carmichael (1987),

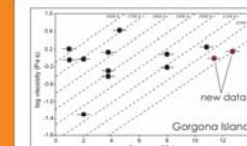


Figure 5a. Viscosities of komatiite liquid from Gorgona Island between 1 and 13 GPa. We observe a positive pressure dependence and measured a positive activation volume of 5 cm<sup>3</sup> mol<sup>-1</sup>. New data from Shing-8 are shown in red.

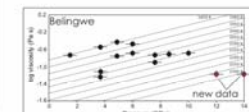


Figure 5b. Viscosities of komatiite liquid from Beilngwe, Zimbabwe between 1.5 and 14 GPa. A similar positive pressure dependence is observed, between 1.5 and 12 GPa with an activation volume of 2.9 cm<sup>3</sup> mol<sup>-1</sup>. The pressure dependence changes, however between 12 and 14 GPa.

### DISCUSSION

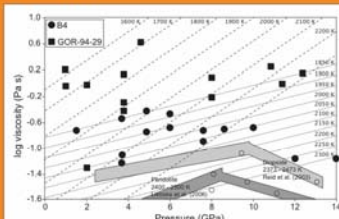


Figure 6. Positive pressure dependences are observed for all depolymerized liquids - komatiite (this work), peridotite (Liebske et al. 2006) and diopside (Reid et al. 2003). Peridotite and diopside viscosities increase up to 8.5 GPa and 10 GPa respectively, before decreasing at higher pressures. Komatiite viscosities may show changes in pressure dependence at higher pressures.

The more polymerized komatiite from Gorgona Island has the highest viscosities and the highest pressure dependence, while the more depolymerized komatiite liquid exhibits the lowest viscosities. Neither Gorgona Island nor Beilngwe liquid viscosities reach maxima < 13 GPa and < 14 GPa, respectively. From our data, one could interpret a change in the pressure dependence of the Beilngwe melt viscosity at 14 GPa. From peridotite and diopside liquid viscosities, we have

observed that maxima occur at higher pressures the higher the concentration of network modifiers. Komatiite liquids follow the same trend, viscosity maxima may be present in these komatiite melts at pressures beyond those of this study. However, our results to 14 GPa agree primarily with those of molecular dynamics simulations.

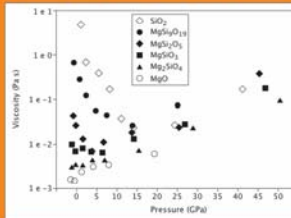


Figure 7. Viscosities of liquids along the SiO<sub>2</sub>-MgO join at pressure, after Lacks et al. (2006).

Molecular Dynamics (MD) simulations are performed on simple systems involving oxygen and one to two cations (Lacks et al. 2006, de Koker et al. 2008, Adiguad et al. 2008). High pressure viscosity studies have involved more complex, depolymerized liquids. The addition of Ca, in the Reid et al. (2003) study, and other cations, including Al, Fe and Ti, in natural systems (this study) may contribute to structural changes that change the physical properties of the liquids. The interaction and mixing of cations (Allwardt et al. 2007) and coordination changes of network modifying cations are not considered in MD simulations, but may account for the changes in the pressure dependence of peridotite and diopside melt viscosities.

### REFERENCES

Adiguad, A., Lacks, D. V., and de Koker, M. 2008. High pressure viscosity studies of simple systems involving oxygen and one to two cations. *Journal of Non-Crystalline Solids* 354: 100-108.

Allwardt, J. R., and Lesher, C. E. 2007. The effect of cation coordination on the viscosity of silicate melts. *Journal of Non-Crystalline Solids* 354: 109-118.

de Koker, M., and Lacks, D. V. 2008. High pressure viscosity studies of simple systems involving oxygen and one to two cations. *Journal of Non-Crystalline Solids* 354: 100-108.

Lange, R. A., and Carmichael, W. M. 1987. Densities of silicate liquids: A review. *Journal of Non-Crystalline Solids* 88: 1-14.

Liebske, D. C., and Reid, J. R. 2006. Viscosities of peridotite and diopside melt. *Journal of Non-Crystalline Solids* 354: 109-118.

Reid, J. R., and Liebske, D. C. 2003. Viscosities of peridotite and diopside melt. *Journal of Non-Crystalline Solids* 354: 109-118.

Terasaki, H., and Lesher, C. E. 2001. Viscosities of komatiite liquids at high pressures. *Journal of Non-Crystalline Solids* 288: 1-14.

Vohrer, P., and Lesher, C. E. 1987. Density of komatiite liquids at high pressures. *Journal of Non-Crystalline Solids* 88: 1-14.

### ACKNOWLEDGEMENTS

This work is largely supported by NSF Grant EAR 05-08222. We thank the staff of the SPiNG-8 beamline at the Advanced Photon Source for their assistance during the experiments. We also thank the staff of the BLD481 beamline at the Advanced Photon Source for their assistance during the experiments. We thank the staff of the BLD481 beamline at the Advanced Photon Source for their assistance during the experiments.

Lara O'Dwyer Brown  
Charles E. Lesher  
Hidenori Terasaki